In presenting this dissertation as a partial fulfillment of the requirements for an advanced degree from the Georgia Institute of Technology, I agree that the Library of the Institution shall make it available for inspection and circulation in accordance with its regulations governing materials of this type.

I agree that permission to copy from, or to publish from, this dissertation may be granted by the professor under whose direction it was written, or, in his absence, by the Dean of the Graduate Division when such copying or publication is solely for scholarly purposes and does not involve potential financial gain.

It is understood that any copying from, or publication of, this dissertation which involves potential financial gain will not be allowed without written permission.

Richard John Veenstra

ANALYSIS OF A CYLINDRICAL SPACE FRAME

A THESIS

Presented to

the Faculty of the Graduate Division

Georgia Institute of Technology

In Partial Fulfillment

of the Requirements for the Degree

Master of Architecture

By

Richard John Veenstra

April 1957

6 12

ANALYSIS OF A CYLINDRICAL SPACE FRAME

Approved: _____

_____

_____

Date Approved by Chairman: April 9, 1957

To my wife,

ALYCE JUNE VEENSTRA

ACKNOWLEDGMENTS

I wish to express my sincerest thanks to Dr. D. A. Polychrone for the initiation of the problem and for the assistance and encouragement given of both a tangible and intangible nature. I should also like to thank Dr. F. W. Schutz and Professor C. M. Gailey, who served on the reading committee, for their assistance and recommendations. A special note of appreciation is due Mr. E. A. Moulthrop and the Robert and Company Incorporated for the financial assistance given.

TABLE OF CONTENTS

LIST OF FIGURES

LIST OF TABLES

ANALYSIS OF A CYLINDRICAL SPACE FRAME

(49)

By: Richard John Veenstra

Advisor: Dr. D. A. Polychrone

This study comprises the first phase of a research program for investigation into the analysis of cylindrical space frames. The results reported are restricted to the structural behavior at the mid-span section and the deflections for a simply supported structure (with no edge restraints) subjected to a uniform dead load. In order to show the analogies between a cylindrical shell and a cylindrical frame, an analytical method based on shell theory is compared with the results of a model analysis.

The analytical method presented utilizes tables from the American Society of Civil Engineers, Manual No. 31. Simplifying assumptions are made to convert the stress patterns of the shell into concentrated forces for the frame members.

A model, constructed of plastic tubes with plywood end diaphragms, is tested by loading a weight at each panel point to simulate a uniform dead load distribution. The strains are measured by SR-4 electric gages, and are recorded for a change from a loaded to an unloaded condition. Deflections of the model under load are obtained by means of dial indicators and a telescope level.

The results of this initial stage demonstrates the merit of the procedure. Particularly good correlation (maximum error of 20 per cent) is obtained for the longitudinal (T_x) stresses. The transverse stress and bending moment (T_ϕ and M_ϕ) are over estimated, although the stress pattern is similar. This is to be expected, due to the lack of similarity

between transverse and longitudinal stiffness of the space frame.

It is recommended that the experimental investigation be continued and studies made of:

1. Restraint of edge members.
2. Change of joint stiffness.
3. Simple support of longitudinal members.
4. Change of diaphragm rigidity.

In addition, analytical studies should be made into the effect of such parameters as transverse versus longitudinal stiffness and relative moments of inertia between a shell and a space frame.

Approved: _____

Date of Approval: April 8, 1957

CHAPTER I

INTRODUCTION

There is a great need for a simplified method of space frame analysis. At present, the methods used for an analysis of this type are very laborious. A space frame is a highly indeterminate structure, and it is impracticable to assume that the joints are free of moments. However, if an analogy between a frame-work and a membrane can be established, theories and solutions for the latter can be utilized. Varied evidence indicates that the structural behavior of a frame-work is analogous to that of a shell.

A cylindrical space frame has the same general shape (see Figure 1) as a concrete shell. This fact alone suggests that their structural behavior will be similar. If such is the case, it seems reasonable that shell solutions can be used as an aid in the analysis of space frame.

The possibilities of using a frame-work to replace a solid shell have not been fully realized. Only a few engineers, such as Edwardo Torroja of Spain and Pier Nervi of Italy, have exploited the advantages of this type structure (see Bibliography).

There is an infinite variety of forms which a space frame might take. However, a cylindrical shape exhibits characteristics which give it great promise in the field of architecture. This shape, for example, facilitates the following:

(a) Adaptability to a rectangular bay system

(b) Application of standard roofing materials

(c) Repetition of the same size members

(d) Roof drainage

(e) Ease of erection

(f) Simplicity (joint detail and fabrication)

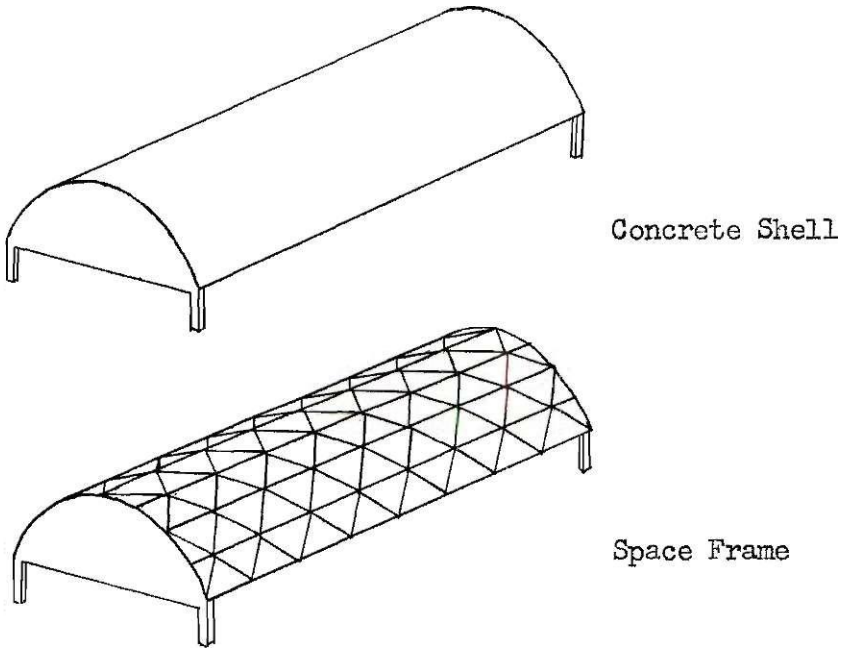

Figure 1. Similarity of Shell and Space Frame

The study made in this thesis comprises the first phase of a research program into the analysis of cylindrical space frames. The particular frame-work chosen for this study is based on an example problem in the American Society of Civil Engineers, Manual No. 31, Design of Cylindrical Concrete Shell Roofs. This will enable the reader who is unfamiliar with the design procedures used in this manual to more readily follow the shell analysis method presented here.

This initial investigation into the analogous structural behavior of a shell and a space frame will be limited to a study of the stresses at the mid-span section and the deflections. The structure is simply supported

with no edge restraints. One load condition, that of a uniform dead load, is analyzed. Simplifying assumptions are made to convert the stresses obtained by the shell theory into components of axial force and bending moments for the frame members. The resulting solution is compared to the values obtained by a model analysis.

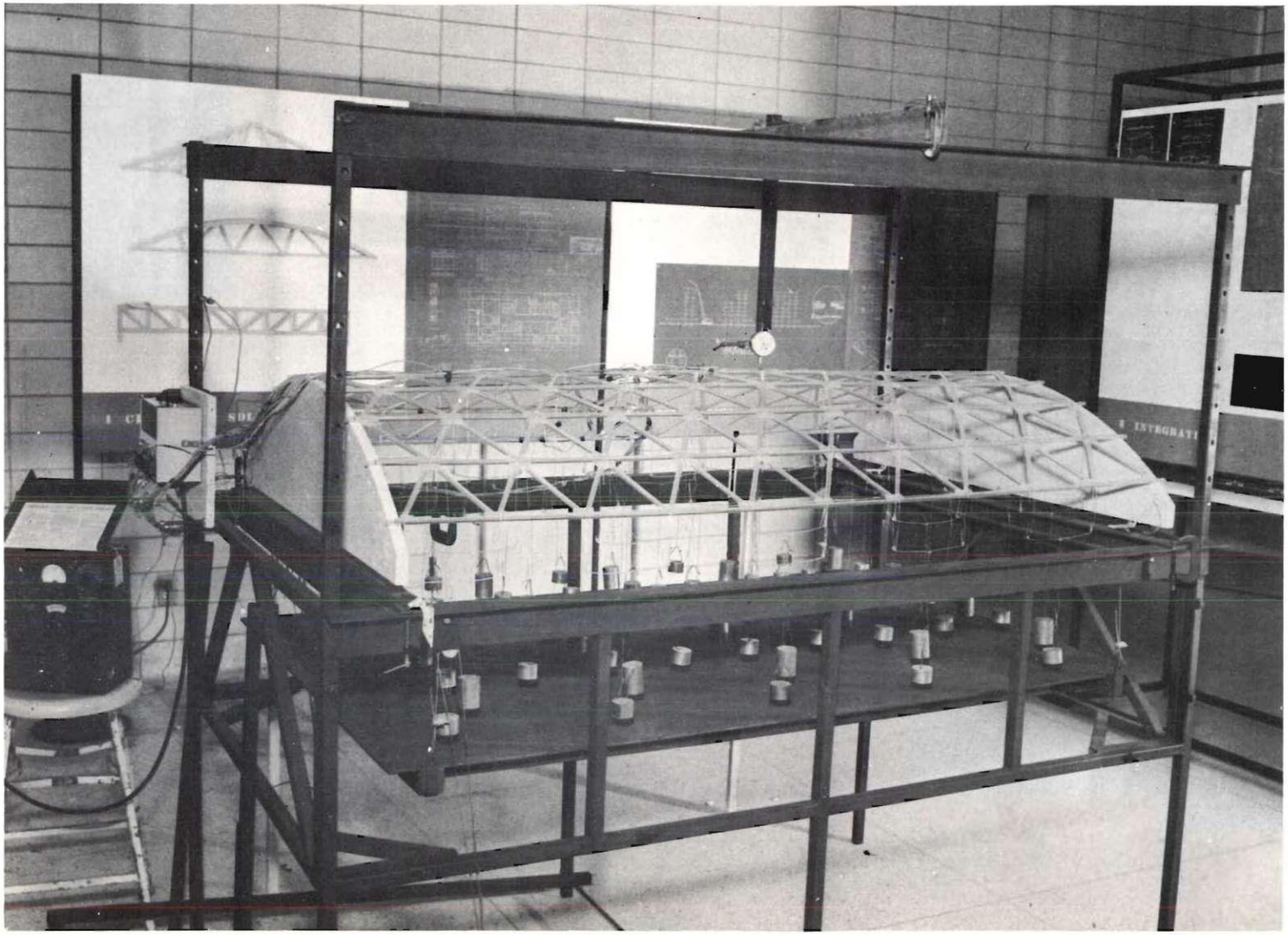

Figure 2. Side View of Model and Test Frame.

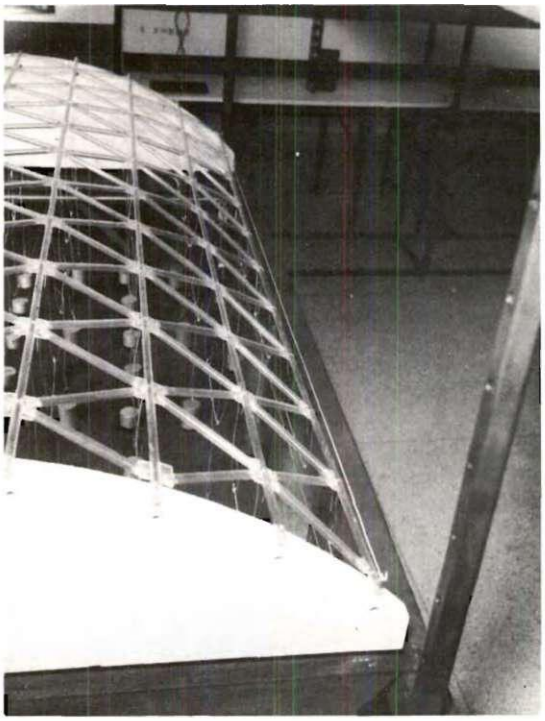

Figure 3. Top View of Model Showing Deflection Under Load.

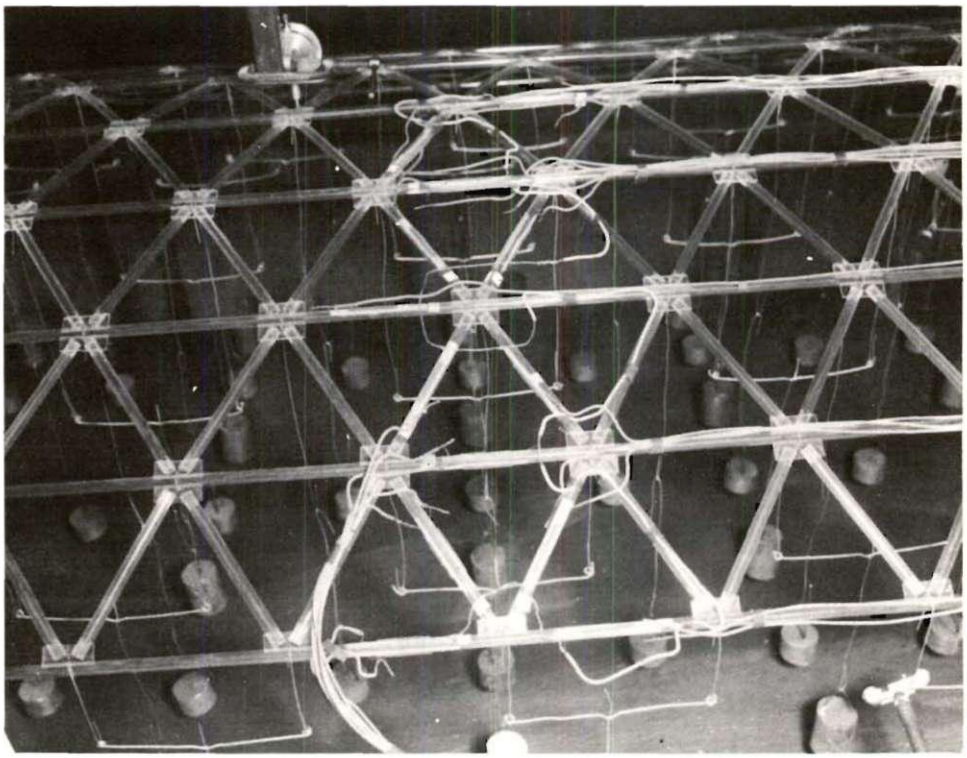

Figure 4. View of SR-4 Gages on Test Model.

CHAPTER II

INSTRUMENTATION AND EQUIPMENT

A model was chosen on the basis of the dimensions given for an example shell problem in the American Society of Civil Engineers Manual No. 31, page 48. The scale of 1" = 1' - 0", was used to facilitate comparison between this study and the figures and examples given for the shell problem in Manual No. 31. The space frame essentially divides the shell into ten longitudinal and eight transverse sections. The resulting dimensions for individual members allow reasonable $\frac{\ell}{r}$ ratios. Plastic was used for the model because of ease of fabrication and a low modulus of elasticity, which would allow large strains under light loads. The end diaphragms were made of plywood. These were considered as infinitely rigid. The gusset plates and tubes are fastened together by Duco cement. Figure 5 shows the model and its dimensions.

Descriptive Information for the Test Model

Dimensions:

Item	Symbol	Dimensions
Span	ℓ	62.0"
Radius	r	31.0"
Width	b	39.8"
Arc length	s	43.3"
Applied load	ω	0.0142 psi

Material:

Plastic - Methacrylate
3/8" O.D. Tube and 0.1" sheet (gussets)

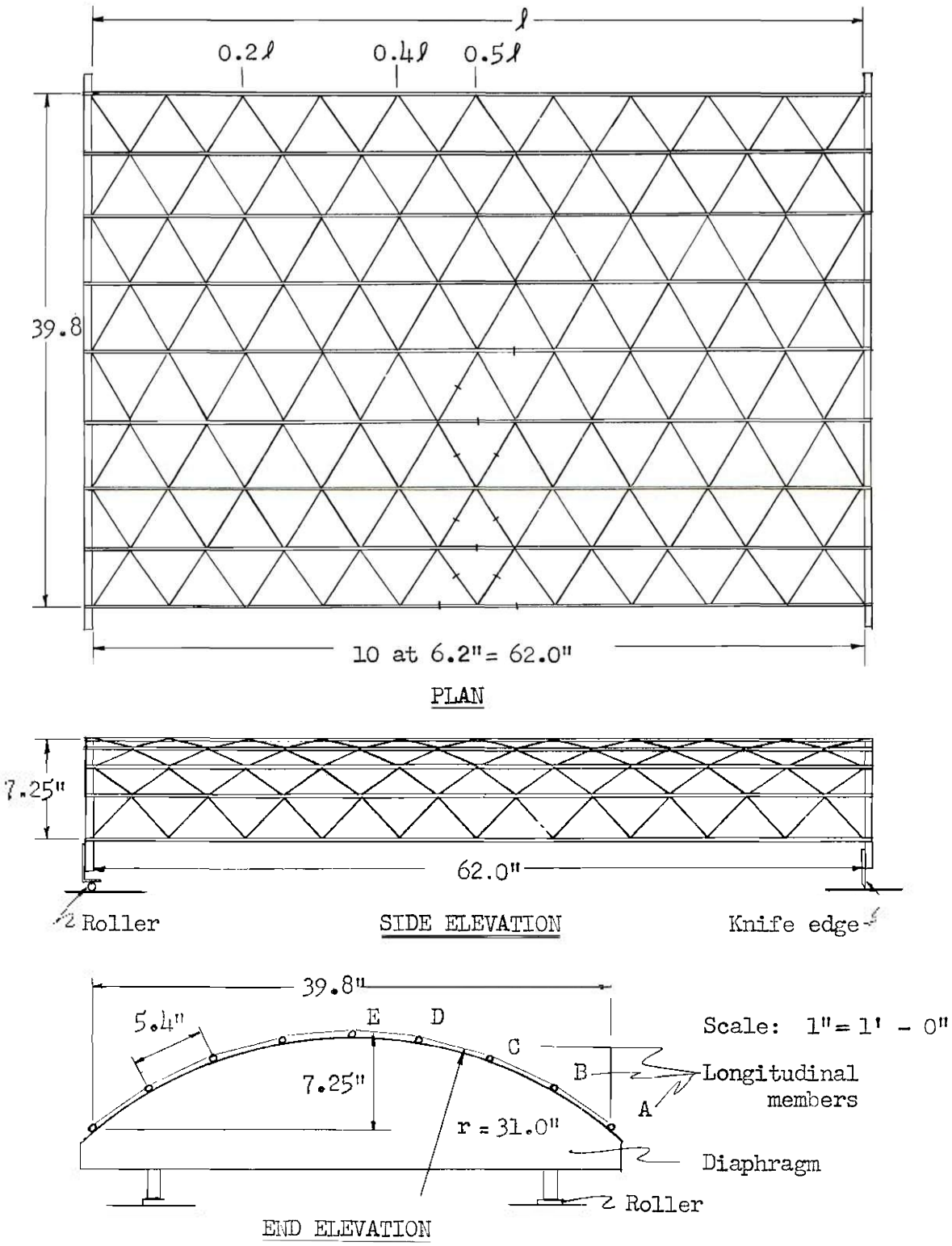

Figure 5. Test Model

Physical Properties of Plastic Tube:

Item	Symbol	Units
Outside diameter	O.D.	3/8"
Inside diameter	I.D.	1/4"
Area	A	0.0614 sq. in.
Moment of inertia	I	0.000779 in. ^{4}
Section modulus	Z	0.004155 in. ^{3}
Modulus of elasticity		
initial	E_o	470,000 psi
after loss	Ef	430,000 psi
Length of members	a	6.2"
Radius of gyration	r	0.05078"
Ratio of $\frac{\ell}{r}$	$\frac{a}{r}$	121.6

Tests to Determine the Modulus of Elasticity and Creep of Plastic

Standard tension tests were used to determine the modulus of elasticity of the plastic tubes. The results of these tests are shown in Figures 13, 14, and 15. In addition, time versus stress was plotted to gain knowledge of the creep characteristics of the material (see Figure 16).

SR-4 Strain Gages

Wire gages, type A-12 (gage factor = 2.05 ± 1%, lot no. B-32) as manufactured by the Baldwin-Lima-Hamilton Corporation, were used to measure strains. Generally, two gages were mounted on each member at the section along the center line of the model. Only one side was instrumentated due to the symmetrical loading. The gages were mounted in two types of orientation, one plane of orientation being in a radial direction, and the other in a tangential direction to the surface. Figure 6 shows the location of the strain gages and their orientation.

Strain Indicator

A Baldwin, type M, (serial no. 362413) SR-4 portable strain indicator was used to read strain increments. The strain indicator was battery operated.

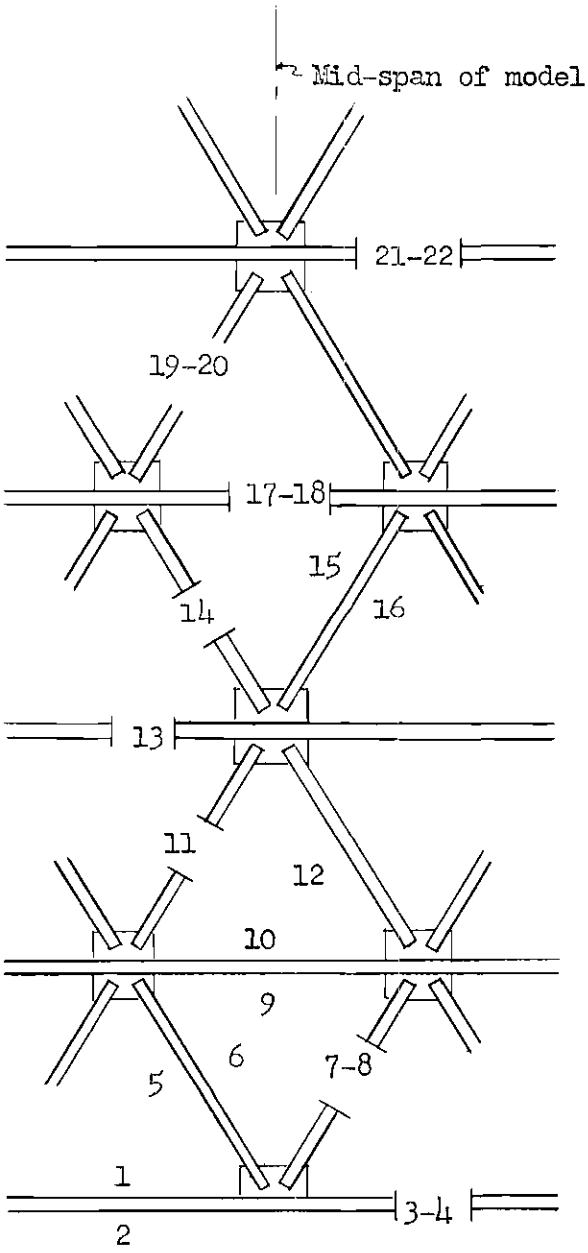

Key:

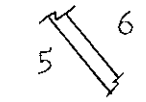

indicates gages mounted in tangential plane

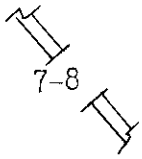

indicates gages mounted in radial plane
(gage 7 is on top surface)

Figure 6. Location and Orientation of SR-4 Gages

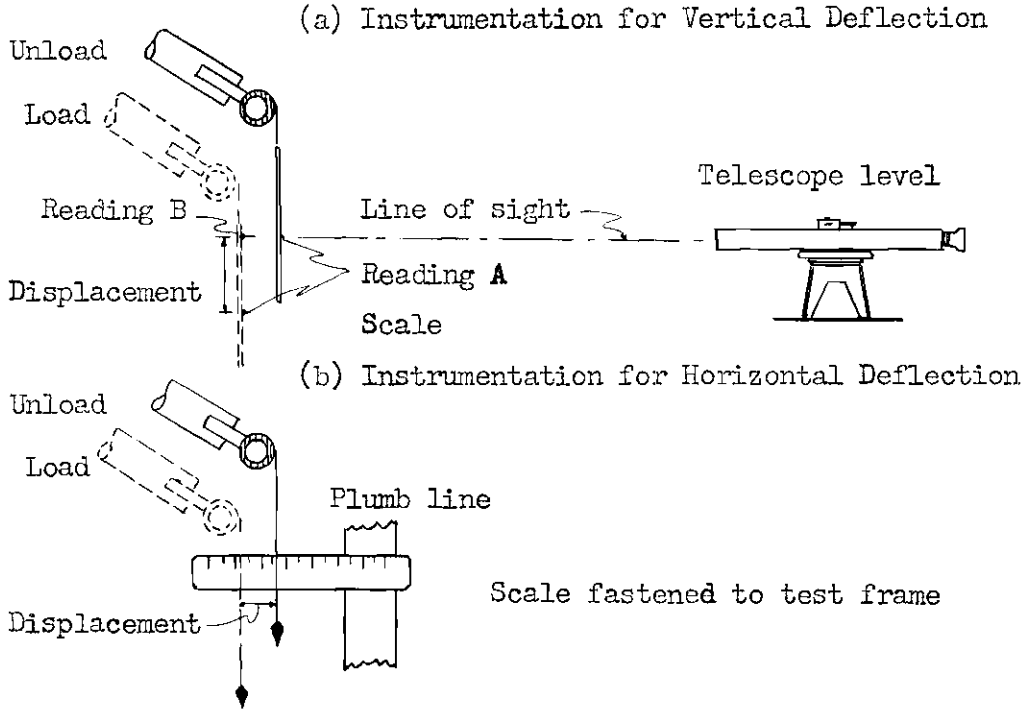

Figure 7. Measuring Deflections of Edge Member

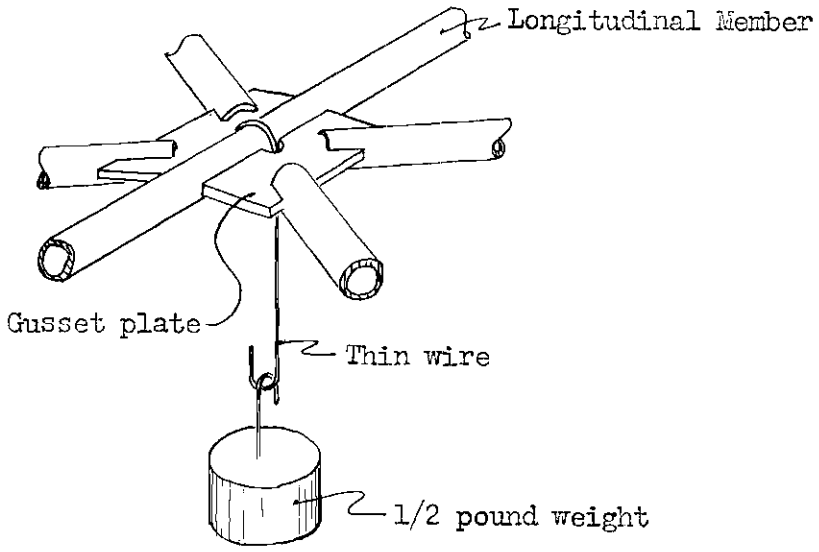

Figure 8. Method for Attaching Weights

CHAPTER III

ANALYSIS PROCEDURE

Because this study is intended to be an initial investigation into the analogy between a space frame and a thin shell, no exact mathematical derivations or solutions will be given. A negative sign (-) is used to indicate compressive strains and forces. The procedure below is based on reasonable simplifying assumptions.

Tables 14 and 15 show the results for shell stress solutions as given in Manual No. 31. There are two solutions, one for a shell having a $\frac{r}{t}$ ratio of 100, and the other for a $\frac{r}{t}$ ratio of 200. The author realizes that herein lies an analogy on which a great amount of investigation must be done in order to establish a definite relation. Perhaps, when further studies have been made, a more suitable parameter will be found. No method is presented here for calculating an equivalent thickness (t) for the space frame. The longitudinal stiffness of the space frame is greater than the transverse stiffness. By inspection of the longitudinal cross section, it is assumed that the values for the longitudinal forces (T_x) will follow more closely the stress pattern developed by the $\frac{r}{t} = 100$ ratio.

Conversion of T_x Forces

The largest forces in the shell will be those due to T_x values. These forces are the ones which resist the longitudinal bending moment induced by the load on the structures. Figure 10 shows the results of Table 14 plotted and subdivided on a developed surface of the shell. The reader may refer to page 50, Manual No. 31, to see the distribution of force on a vertical plot. Note that values for the plot in Figure 10 are for a unit load of 1 pound per square inch.

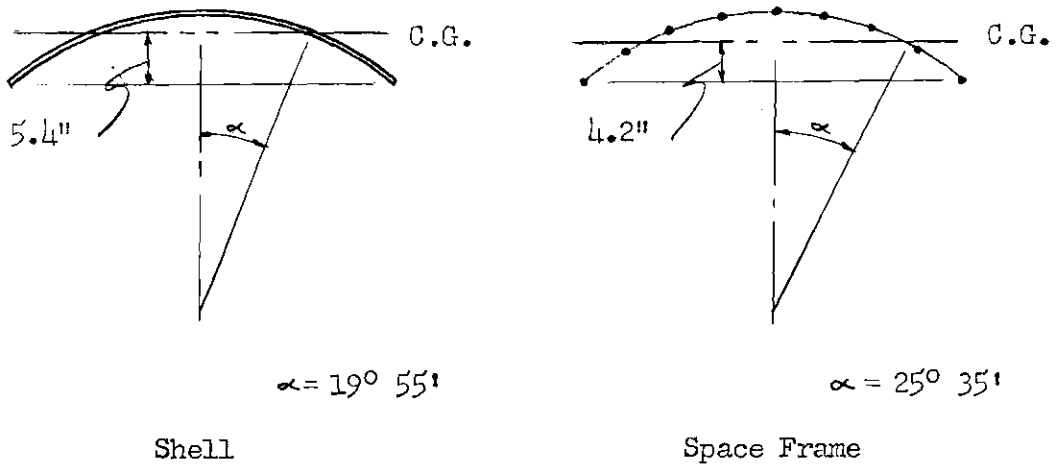

Figure 9. Location of Center of Gravity

The location of the center of gravity of the space frame differs from that of the shell (see Figure 9). Although the stress distribution is not a straight line, we can expect that a relative shift downward will occur. This shift can be estimated by assuming the mass of the frame to be concentrated at the locations of the longitudinal members. The effect of this movement on the values of T_x is shown in Figure 10.

Due to the rigid construction of the joints, the diagonal members can carry part of this T_x force. For this illustration, it is assumed that they could carry 20 per cent of the load area. This segment of load is assumed to be midway between each successive pair of longitudinal members. The force in the member is now considered to be the area (cross-hatched) remaining under the curve on either side of the individual members.

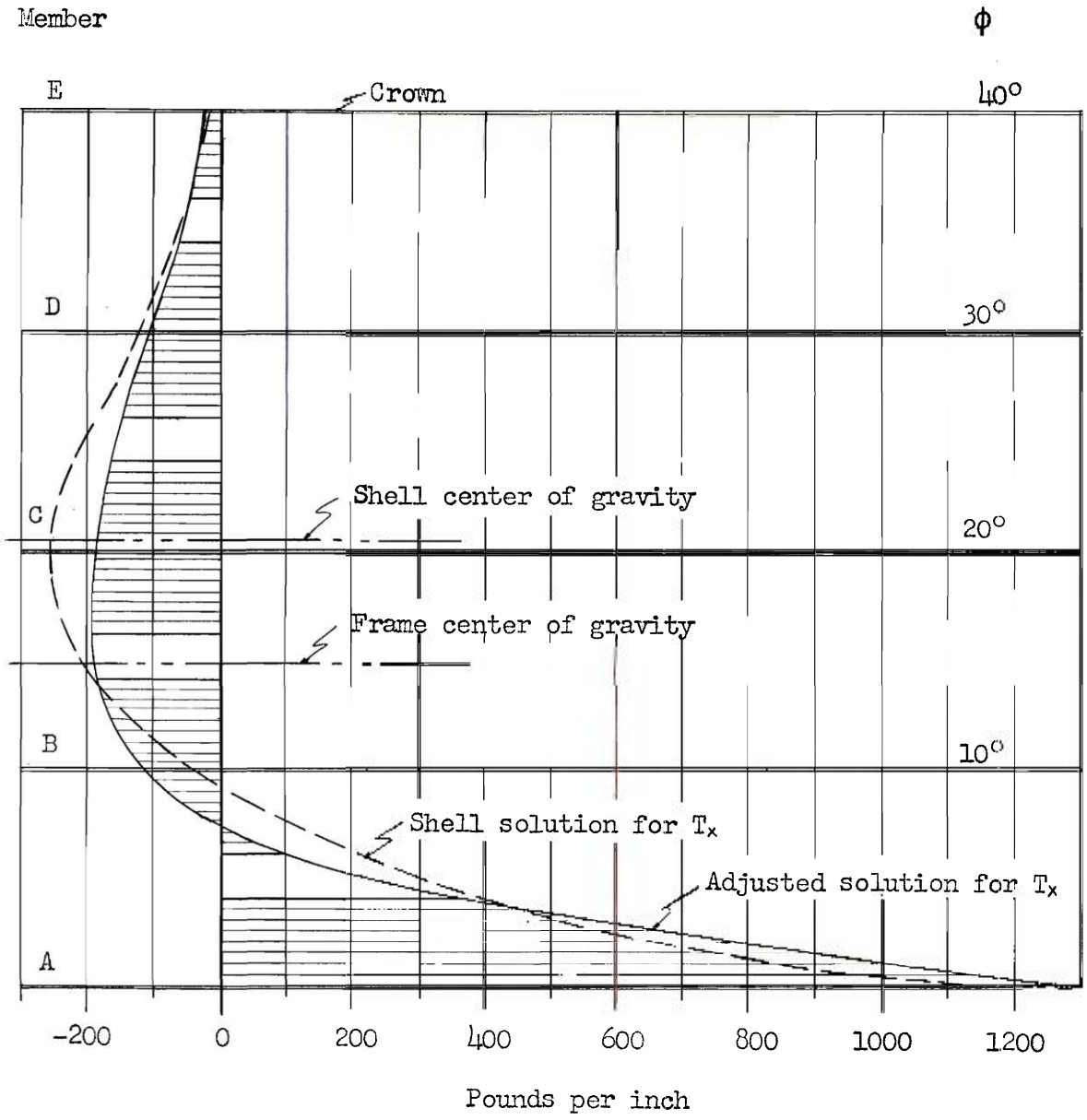

Figure 10. Values of T_x Based on Shell Theory

The area is then multiplied by the load (0.0142 psi) to yield the expected force in each member. The resulting forces are given below in Table 1. The longitudinal members are lettered alphabetically from the bottom (A) to the crown (E).

Table 1. Force in Longitudinal Members Caused by T_x

Longitudinal Member	Area	X	Load	=	Axial Force (pounds)
E	86		0.0142		-1.22
D	432		0.0142		-6.14
C	833		0.0142		-11.82
B	443		0.0142		-6.28
A	1950		0.0142		27.65

(- indicates compression)

Conversion of T_ϕ Forces

The T_ϕ force at this section of the shell can be estimated by the same method as used for T_x. It should be kept in mind that the shear value, S, is equal to zero at the center line. Assume again a 20 per cent loss due to rigid joints. As the T_ϕ curve is relatively flat (see page 50, Manual No. 31), average values can be estimated for Table 2 without drawing a plot. The values given in Tables 14 and 15 are for positions related to ϕ ($\phi = 0, \phi = 10, \phi = 20$, etc). Since the longitudinal members are spaced at ten degree intervals, these values correspond to the positions of the longitudinal members (A, B, C, D and E). The values of T_ϕ are given in pounds per inch; therefore, it is necessary to multiply this by the equivalent horizontal length over which the member acts (3.1 inches in this case). In addition, the longitudinal members are assumed to carry 20 per cent of the load. Since the values of T_ϕ given in Tables 14 and 15 are

for a unit load, a correction must be made by multiplying by the actual load of 0.0142 pounds per square inch. The above will yield the vertical component of the force in the diagonal members. The estimation of this force is shown below, and is given for the diagonal members between the longitudinal members indicated at the left.

Table 2. Estimation of Force from T_ϕ

Longitudinal Member		$\frac{r}{t} = 100$			$\frac{r}{t} = 200$		
		T_ϕ	Mult.	Force (pounds)	T_ϕ	Mult.	Force (pounds)
(Crown)	E						
		53.5	x 0.0408	= -2.70	40.9	x 0.0408	= -1.67
	D						
		48.7	x 0.0408	= -1.99	48.1	x 0.0408	= -1.96
	C						
		32.1	x 0.0408	= -1.31	42.4	x 0.0408	= -1.73
	B						
		9.9	x 0.0408	= -.40	16.5	x 0.0408	= -.67
	A						

(Multiplier: $\frac{6.2}{5.4}$ x 3.1 x .8 x 0.0142 = .0408)

Conversion of M_ϕ Forces

The value of the bending moment caused by M_ϕ on the diagonal members can be estimated as follows in Table 5. The values given for M_ϕ in Tables 14 and 15 are in inch pounds per inch; therefore, these must be multiplied by 3.1 inches (the horizontal distance the diagonal member covers). As in the case of T_ϕ, the unit load value must be converted by using the actual load of 0.0142 pounds per square inch.

Table 3. Estimation of Moment from M_ϕ

Longitudinal Member		$\frac{r}{t} = 100$			$\frac{r}{t} = 200$		
		M_ϕ	Mult.	Moment (inch pounds)	M_ϕ	Mult.	Moment (inch pounds)
(Crown)	E						
		32.0	x 0.044	= - 1.41	16.0	x 0.044	= - .70
	D						
		24.5	x 0.044	= - 1.08	16.5	x 0.044	= - .73
	C						
		10.6	x 0.044	= - .47	11.1	x 0.044	= - .48
	B						
		1.5	x 0.044	= - .07	3.0	x 0.044	= - .13
	A						

(Multiplier: 3.1 x 0.0142 = 0.044)

Calculation of Edge Deflection

The horizontal and vertical displacement of the edge can be calculated by using table 1B and 2B, of Manual No. 31. If the constant, E, is held out of the calculation, the results at the center line are as follows:

$$\Delta V = \frac{28,400}{E}$$

$$\Delta H = \frac{13,900}{E}$$

If a modulus of elasticity of 450,000 psi is used, the result becomes:

ΔV = .061" (downward deflection)

ΔH = .030" (inward deflection)

Figure 12 shows the deflection curve for the shell theory.

CHAPTER IV

TESTING PROCEDURE

Strain Gage Readings for Model Test

Two types of loading cycles were used while taking strain readings. A short cycle test was used to expedite readings and also to check the feasibility for using this method with plastic. With this type test, the unload reading is taken, and then the load applied. The load reading is taken as rapidly as the strain indicator can be balanced. This generally requires about five to ten seconds. The results of these tests (1, 2, 3, and 4) are given in Tables 9, 10, 11, and 12. In order to obtain a more accurate answer, the results of all the short cycle tests are averaged in Table 4, below.

Table 4. Average Axial Strain Gage Readings for Short Cycle Tests

(- indicates compression)

Gage No.	Strain (microinches)	Gage No.	Strain (microinches)
1.	873.5	10.	-188.1
2.	770.0	11.	-68.8
3.	611.9	12.	-38.1
4.	1035.6	13.	-353.1
5.	.6	14.	110.6
6.	15.0	15.	-33.1
7.	-55.6	16.	-27.8
8.	56.9	17.	-196.3
9.	-153.1	18.	-185.0

Gage No.	Strain (microinches)	Gage No.	Strain (microinches)
19.	200.6	21.	-55.6
20.	-268.8	22.	-107.5

In addition to the short cycle tests, a long time load test was made. This test consisted of taking and reading all of the unload readings before application of the load. Time was allowed (approximately 15 minutes per gage) for all movement of the indicator to cease before a reading was taken. The major cause of this instrument drift (when testing plastic models) is believed to be due to local temperature change as electric current is passed through the gage (although creep of the plastic may add some effect, particularly in the load readings). However, the movement is slight, and readings could be taken without this delay. The load was then applied and remained on the model for approximately five hours before the load readings were made. This time interval allowed nearly all creep to take place (see Figure 16) before final strains were recorded. The results of this test are given in Table 13.

Figure 16 indicates that the increase in strain for this test over initial strain would be about nine per cent. Therefore, in order to compare the results of short cycle and long time load tests, proportionate reduction is made of the values in Table 13 and the results listed in Table 5 below. These values are shown as an 8.5 per cent reduction in strain. This corresponds to a 9.0 per cent increase in the modulus of elasticity. In other words, the modulus of elasticity varies (due to creep) from about 470,000 psi to 430,000 psi.

Table 5. Strains for Long Time Load Test with 8.5 per cent Reduction

Gage No.	Strain (microinches)	Gage No.	Strain (microinches)
1.	878.4	12.	-36.6
2.	768.6	13.	-375.2
3.	627.7	14.	94.2
4.	1028.5	15.	-36.6
5.	0.	16.	-27.5
6.	13.7	17.	-214.1
7.	-60.4	18.	-183.0
8.	56.7	19.	210.5
9.	-153.7	20.	-279.1
10.	-199.5	21.	-60.4
11.	-78.7	22.	-115.3

Bending and Axial Strains

Members in the space frame are subjected to bending as well as axial strains. Figure 11 shows the strain distribution occurring in the members. To the right of the strain diagrams in Figure 11 are values for the resulting axial force and bending moment.

Huggenberger Strain Readings

After the tests using the SR-4 gages were completed, Huggenberger strain gages were used at various points to corroborate the results of the SR-4 readings. Although Huggenbergers are not as sensitive as SR-4 gages, they were utilized to check any errors in reading or defects in the SR-4 gages.

Deflection of the Model

The displacements of the model are the average of the four deflection readings (see Figure 12). It can be seen that the crown member (E) deflected upward. This is due to the fact that the increase in rise (caused by a shorter radius of curvature of the section) exceeded the total downward edge deflection.

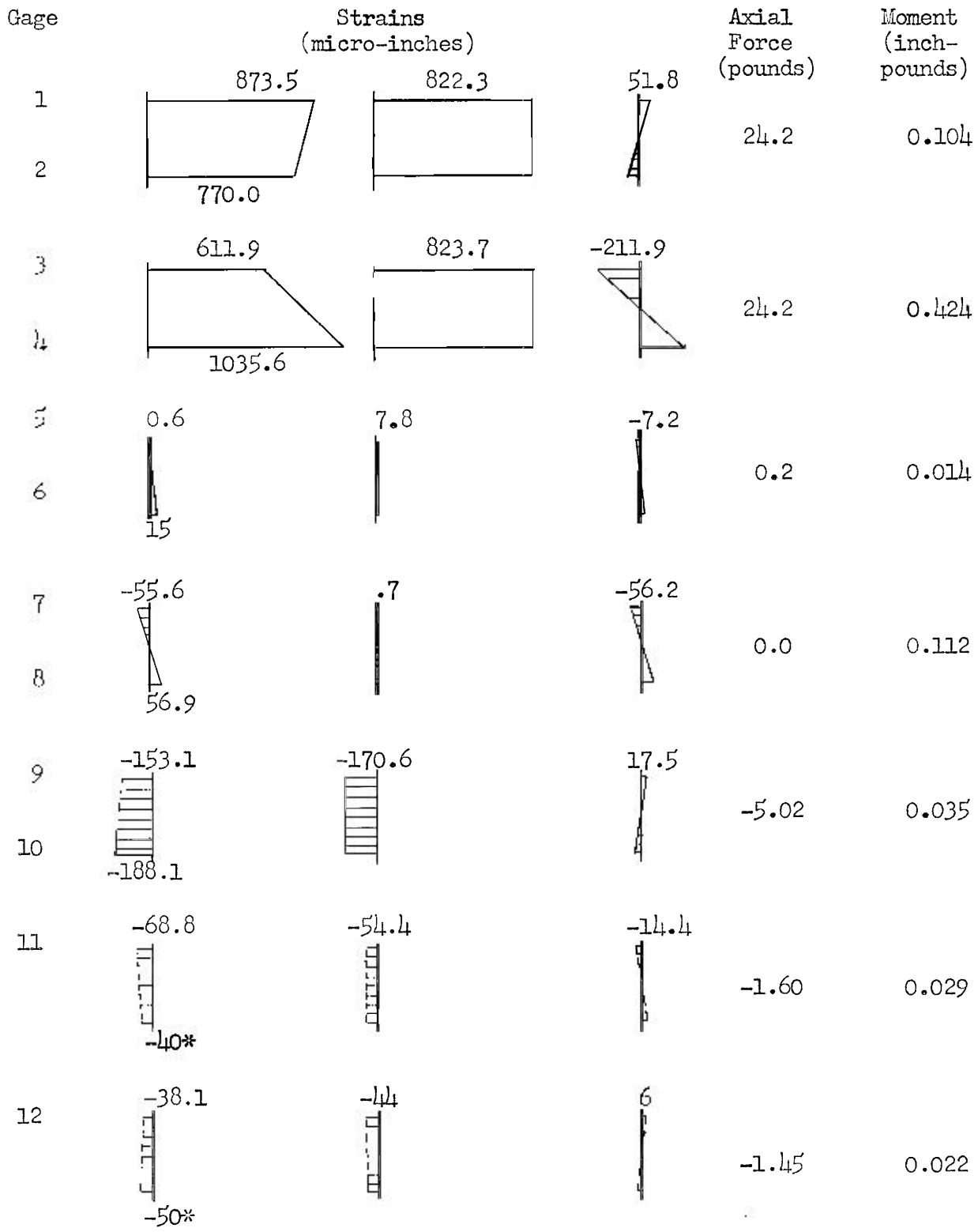

Figure 11. Axial Force and Bending Moments of Members

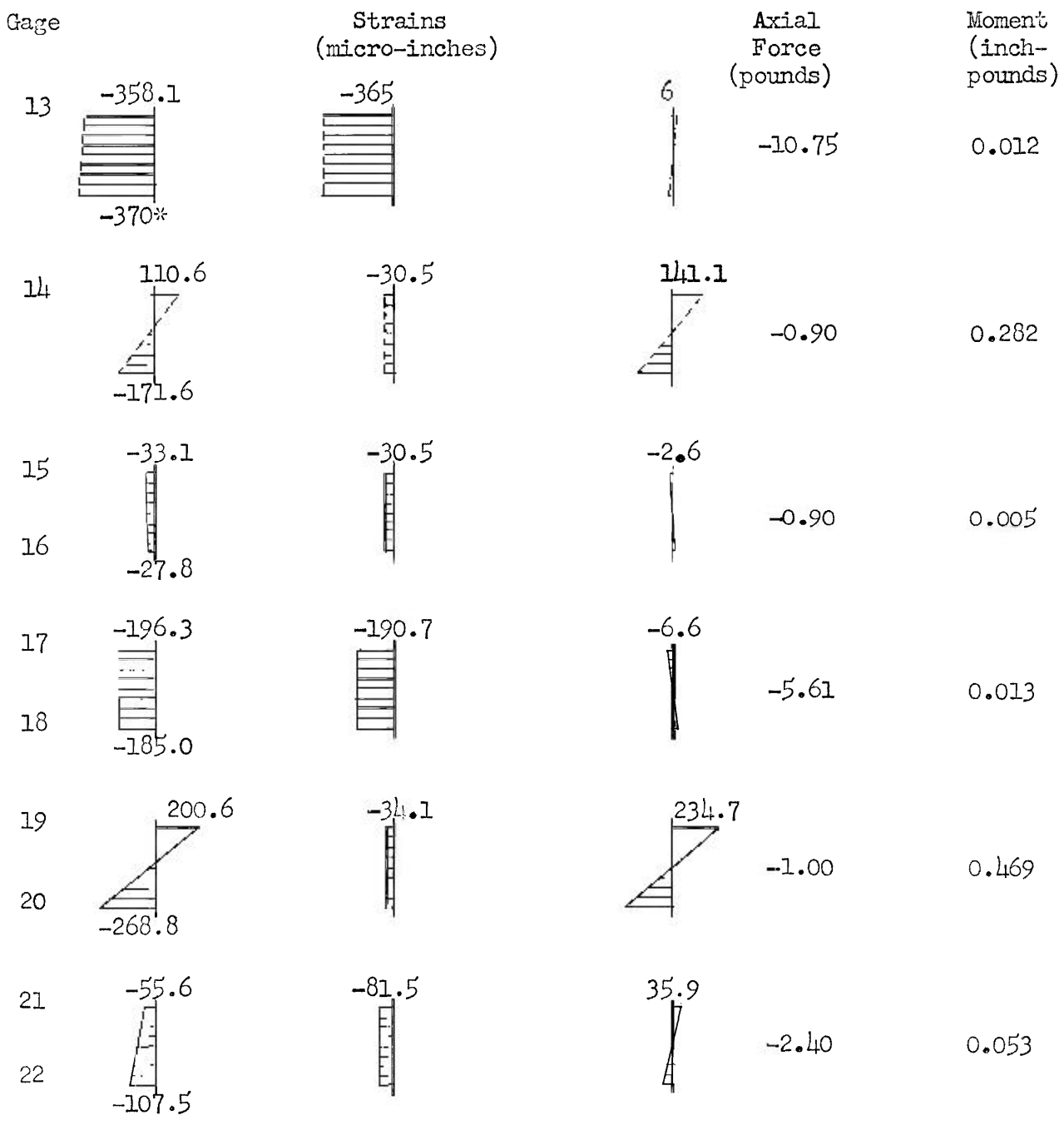

Figure 11. Continued

CHAPTER V

DISCUSSION OF RESULTS

Comparison of T_x Forces

Table 6 lists the values for the forces in the longitudinal members obtained by conversion of shell stresses and those obtained by the model analysis.

Table 6. Comparison of T_x Forces

	Analogous Shell	Model
Member	Axial Force	Axial Force
E	-2.44	-2.40
D	-6.14	-5.61
C	-11.82	-10.75
B	-6.28	-5.02
A	27.65	24.2

The results above indicate that a reasonable prediction of the axial forces in the longitudiral members was obtained.

Another check on the results can be made by calculating the internal moment, which is produced by the forces.

Force	X	Arm	Moment
2.40		7.25	17.4
2 x 5.61		6.78	76.0
2 x 10.75		5.38	115.5
2 x 5.02		3.10	31.1
2 x 24.20		0.	0.
			240.0 pound inches

Sum

$M = \frac{W l^2}{8}$ $\qquad W = 43.4 \times 0.0142 = 0.614$

$M = \frac{0.614 \times 62 \times 62}{8} = 295$ pound inches

From the above calculation, it is evident that the longitudinal members carry approximately 80 per cent of the moment. Therefore, it seems that the remaining 20 per cent is taken by the diagonal members. For this particular case, it shows that the original assumption was a reasonable estimate. These results are by no means to be considered as a proof, but as an indication of the possibility of utilizing shell solutions to study the forces in an analogous space frame.

Comparison of T_ϕ Forces

The values for axial force in the diagonal members due to T_ϕ are all lower than the shell solution indicated. Most of this deviation is probably caused by the reduced stiffness (in a transverse direction). The deflections will also indicate this reduction in the analogous modulus of elasticity, as it might be termed.

Table 7. Comparison of T_ϕ Forces

Longitudinal Member	Analogous Shell $\frac{r}{t}=100$	Analogous Shell $\frac{r}{t}=200$	Model
E			
	-2.70	-1.67	-1.00
D			
	-1.99	-1.96	-.90
C			
	-1.31	-1.73	-1.45
B			
	-.40	-.67	-.20
A			

From the above comparison it appears that the model values are about half of the values figured for $\frac{r}{t} = 100$, and follow the same pattern with the exception of the diagonal member between B and C. This axial force was calculated with the aid of a Huggenberger, and therefore, has a greater chance of error.

Comparison of M_ϕ Moments

For a more accurate comparison of transverse moment values, an increase in the moment of the diagonal member should be made. As an estimate, the relative radii of curvatures can be used as a basis for increase. The transverse radius is 31.0 inches and the approximate diagonal radius is 42.0 inches. This would be an increase of 136 per cent. In addition, the variation of change of curvature under load would be greater in the transverse direction.

Table 8. Comparison of M_ϕ Moments

Longitudinal Member	$\frac{r}{t} = 100$	$\frac{r}{t} = 200$	Model
E	-1.41	-.70	-.64
D	-1.08	-.73	-.39
C	-.46	-.48	-.03
B	-.07	-.13	.15
A			

The reversal of moment may well be caused from the fact that the

longitudinal members are fixed to the diaphragm. This effect shows in the deflection results which follow.

Comparison of Deflections

The deflections of the model are much larger than the calculated deflections. The major cause of this variation is the relationship between the modulus of elasticity used in the shell theory formulae, and an equivalent modulus of elasticity which should be used for the frame. No attempt has been made in this study to derive methods for calculating this value. An additional problem arises also from the fact that by replacing a solid material with a framework, it will no longer be isotropic.

A deviation from the theoretical deflection curve at the edge in the model is caused by end fixity of the longitudinal members. This effect is particularly noticeable in the crown and edge members (see Figure 12).

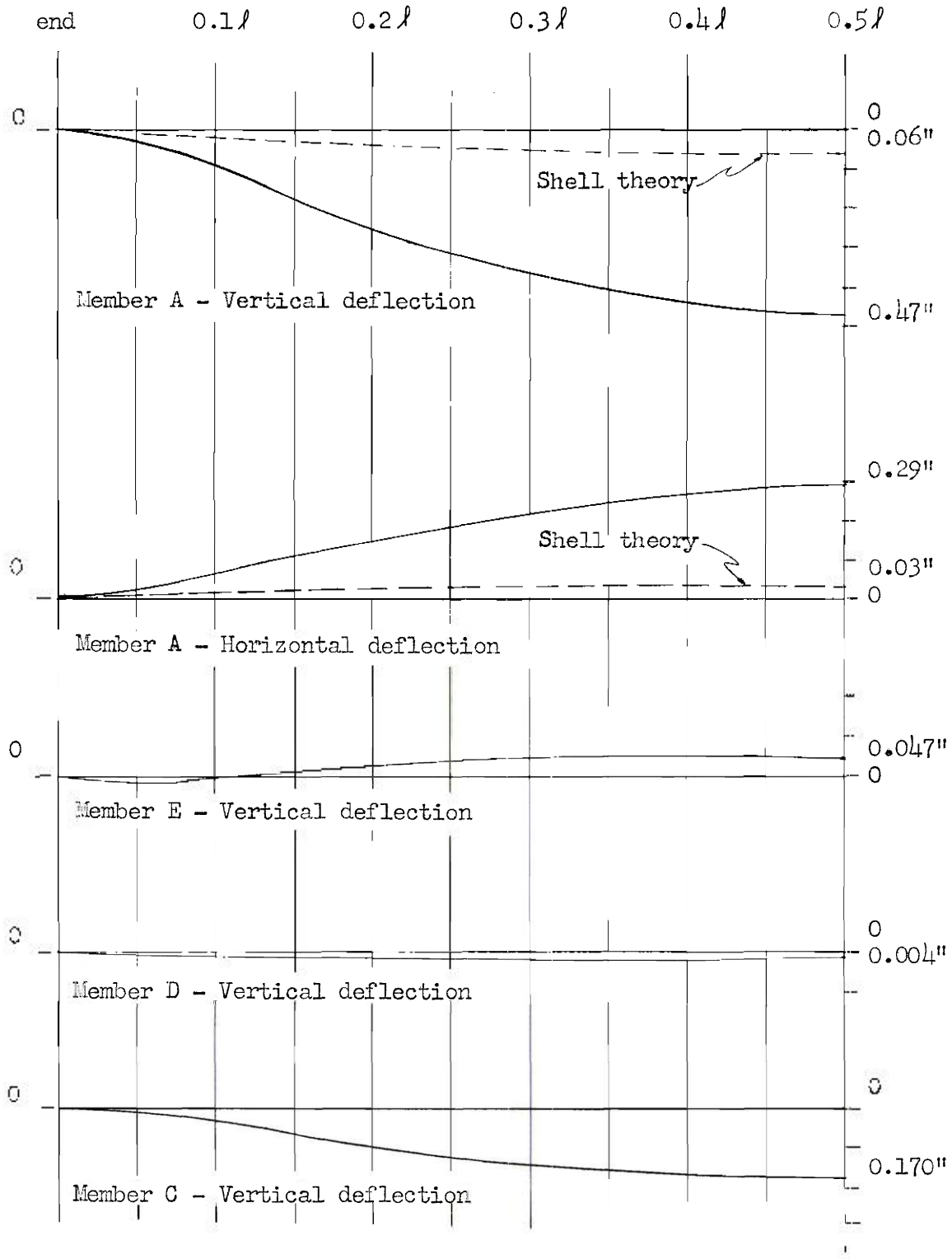

Figure 12. Comparison of Deflections

CHAPTER VI

CONCLUSIONS

The results of this investigation are not intended to be proofs of a theory, but are to serve as an indication of the analogous structural behavior of a shell and a space frame. It should be remembered that data obtained was for one particular space frame. The information contained in this report can be used as a basis for further study, both theoretical and experimental, into the analogies of space frames and shells.

The experimental work carried out in this investigation indicates that:

(a) The basis concept of the structural behavior of the shell and space frame was confirmed.

(b) A reasonable estimate of the longitudinal forces (T_x) was obtained for this space frame by using an analogous shell solution.

(c) The analogous shell solution would be useful in the analysis of a space frame, particularly in the preliminary design stage.

(d) Further experimental investigation into the analogies of shells and space frames is warranted.

CHAPTER VII

RECOMMENDATIONS

Additional tests should be made with the model used for this investigation. The following tests and changes are suggested:

1. The addition of a secondary gusset plate at each joint to increase the transverse stiffness.
2. Horizontal deflections of the edge member restrained to simulate multiple shell condition.
3. Change of the fixed condition of the longitudinal member to a pin condition at the diaphragm.
4. Replacement of rigid diaphragm with diaphragms of varying degrees of stiffness.

Independent investigations (both experimental and analytical) should be made to correlate the analogies between a shell and a space frame. It is suggested that studies be made of the following:

1. The effect of various ratios of transverse to longitudinal stiffness.
2. The value of using an equivalent thickness as a parameter.
3. The variations caused by difference in relative moments of inertia of a shell and a space frame.
4. The effect of joint stiffness.
5. The orthotropic properties of a space frame.

A P P E N D I X

T A B L E S

Table 9. Strain Gage Readings for Test No. 1

Gage No.	1	2	3	4	5	6	7	8
Unload	12062	12300	10990	12500	10860	11955	12550	12320
Load	12940	13085	11600	13540	10860	11970	12500	12390
Change	878	785	610	1040	0	15	-50	70
Unload	12075	12340	11020	12545	10850	11965	12570	12350
Load	12945	13100	11625	13575	10850	11980	12520	12410
Change	870	760	605	1030	0	15	-50	60
Average	874	768	608	1035	0	15	-50	65

Gage No.	9	10	11	12	13	14	15	16
Unload	9880	9600	12200	12460	11790	11810	11250	12130
Load	9725	9420	12140	12430	11440	11920	11220	12100
Change	-155	-180	-60	-30	-350	110	-30	-30
Unload	9895	9620	12220	12480	11800	11825	11270	12140
Load	9750	9430	12150	12445	11450	11930	11235	12120
Change	-145	-190	-70	-35	-350	105	-35	-20
Average	-150	-185	-65	-33	-350	108	-33	-25

Gage No.	17	18	19	20	21	22
Unload	10740	11770	10430	11190	11220	11270
Load	10545	11590	10630	10930	11170	11160
Change	-195	-180	200	-260	-50	-110
Unload	10750	11790	10455	11220	11215	11285
Load	10555	11610	10655	10950	11170	11180
Change	-195	-180	200	-270	-45	-105
Average	-195	-180	200	-265	-48	-108

(Negative indicates compression)

Table 10. Strain Gage Readings for Test No. 2

Gage No.	1	2	3	4	5	6	7	8
Unload	12050	12290	10980	12510	10820	11920	12570	12320
Load	12900	13030	11600	13560	10820	11940	12520	12380
Change	850	750	620	1050	0	20	-50	60
Unload	12060	12330	11015	12560	10840	11940	12585	12350
Load	12920	13090	11625	13560	11840	11960	12530	12410
Change	860	760	610	1000	0	20	-55	60
Average	855	755	615	1025	0	20	-53	60

Gage No.	9	10	11	12	13	14	15	16
Unload	9850	9560	12190	12460	11760	11770	11240	12110
Load	9700	9380	12130	12420	11405	11890	11210	12085
Change	-150	-180	-60	-40	-355	120	-30	-25
Unload	9870	9590	12210	12475	11780	11800	11270	12140
Load	9720	9410	12145	12435	11425	11915	11235	12100
Change	-150	-180	-65	-40	-355	115	-35	-30
Average	-150	-180	-63	-40	-355	118	-33	-28

Gage No.	17	18	19	20	21	22
Unload	10700	11750	10410	11150	11190	11315
Load	10510	11580	10615	10890	11140	11200
Change	-190	-170	205	-260	-50	-115
Unload	10720	11780	10435	11190	11210	11310
Load	10530	11600	10640	10920	11155	11200
Change	-190	-180	205	-270	-55	-110
Average	-190	-175	205	-265	-53	-113

(Negative indicates compression)

Table 11. Strain Gage Readings for Test No. 3

Gage No.	1	2	3	4	5	6	7	8
Unload	12450	12715	11400	12990	11230	12340	12940	12740
Load	13350	13515	12040	14040	11230	12355	12880	12790
Change	900	800	640	1050	0	15	-60	50
Unload	12465	12740	11440	13010	11240	12350	12960	12750
Load	13360	13525	12060	14060	11235	12365	12900	12800
Change	895	785	620	1050	-5	15	-60	50
Average	898	793	630	1050	-3	15	-60	50

Gage No.	9	10	11	12	13	14	15	16
Unload	10240	9980	12560	12810	12130	12140	11610	12500
Load	10085	9790	12490	12770	11770	12250	11580	12475
Change	-155	-190	-70	-40	-360	110	-30	-25
Unload	10255	9990	12570	12820	12150	12160	11630	12515
Load	10100	9795	12495	12780	11785	12270	11595	12488
Change	-155	-195	-75	-40	-365	110	-35	-27
Average	-155	-193	-73	-40	-363	110	-33	-26

Gage No.	17	18	19	20	21	22
Unload	11100	12190	10800	11550	11520	11600
Load	10900	11995	11000	11275	11470	11495
Change	-200	-195	200	-275	-50	-105
Unload	11110	12180	10830	11580	11540	11620
Load	10910	11995	11030	11305	11470	11510
Change	-200	-185	200	-275	-70	-110
Average	-200	-190	200	-275	-60	-108

(Negative indicates compression)

Table 12. Strain Gage Readings for Test No. 4

Gage No.	1	2	3	4	5	6	7	8
Unload	12430	12660	11360	12900	11165	12330	12900	12700
Load	13300	13425	11960	13940	11170	12340	12840	12755
Change	870	765	600	1040	5	10	-60	55
Unload	12450	12700	11400	12950	11180	12340	12940	12720
Load	13315	13465	11990	13975	11185	12350	12880	12770
Change	865	765	590	1025	5	10	-60	50
Average	868	765	595	1033	5	10	-60	53

Gage No.	9	10	11	12	13	14	15	16
Unload	10200	9950	12540	12800	12100	12120	11600	12450
Load	10045	9755	12465	12760	11740	12230	11570	12420
Change	-155	-195	-75	-40	-360	110	-30	-30
Unload	10220	9970	12560	12820	12140	12150	11620	12475
Load	10060	9775	12485	12780	11770	12255	11580	12445
Change	-160	-195	-75	-40	-370	105	-40	-35
Average	-158	-195	-75	-40	-365	108	-35	-33

Gage No.	17	18	19	20	21	22
Unload	11050	12175	10800	11500	11580	11630
Load	10850	11985	11000	11240	11520	11530
Change	-200	-190	200	-260	-60	-100
Unload	11070	12180	10830	11550	11580	11650
Load	10870	11990	11025	11270	11515	11545
Change	-200	-190	195	-280	-65	-105
Average	-200	-190	198	-270	-63	-103

(Negative indicates compression)

Table 13. Strain Gage Readings for Test No. 5

Gage No.	1	2	3	4	5	6	7	8
Unload	12110	12390	11080	12636	10912	12020	12656	12424
Load	13070	13230	11765	13760	10910	12035	12590	12486
Change	960	840	685	1124	-2	15	-66	62
Gage No.	9	10	11	12	13	14	15	16
Unload	9988	9720	12270	12543	11910	11887	11360	11212
Load	9820	9502	12184	12503	11500	11990	11320	12182
Change	-168	-218	-86	-40	-410	103	-40	-30
Gage No.	17	18	19	20	21	22		
Unload	10870	11910	10540	11295	11321	11402		
Load	10636	11710	10770	10990	11255	11276		
Change	-234	-200	230	-305	-66	-126		

(Negative indicates compression)

Table 14. Solution of Shell Stresses for $\frac{r}{t} = 100$

Row	Load	Φ = 40°	30°	20°	10°	0
		Values of T_Φ at $\frac{\ell}{2}$ (pounds per inch)				
1.	None					
2.	Dead	-39.463	-38.863	-37.083	-34.175	-30.229
3.	V_L	-6.956	-20.772	-40.067	-23.589	12.494
4.	H_L	-5.094	8.405	32.764	35.381	17.737
5.	S_L	-2.503	-1.889	.087	2.519	0.
6.	ξ	-54.016	-53.119	-44.299	-19.864	0.
		Values of S at 0 (pounds per inch)				
1.	None					
2.	Dead	0.	-8.721	-17.190	-25.122	-32.297
3.	V_L	0.	86.740	29.419	-136.134	0.
4.	H_L	0.	-87.480	-68.909	47.097	0.
5.	S_L	0.	4.412	-9.095	-5.180	32.297
6.	ξ	0.	-13.873	-65.775	-119.339	0.
		Values of T_X at $\frac{\ell}{2}$ (pounds per inch)				
1.	None					
2.	Dead	-31.981	-31.507	-30.055	-27.687	-24.499
3.	V_L	425.306	109.124	-517.720	-452.820	2030.151
4.	H_L	-396.599	-170.328	308.980	388.634	-1127.185
5.	S_L	-14.766	-18.190	-11.020	54.491	246.491
6.	ξ	-18.040	-110.901	-249.815	-37.382	1124.958
		Values of M_Φ at $\frac{\ell}{2}$ (inch pounds per inch)				
1.						
2.						
3.	V_L	-79.753	-81.560	-75.536	-45.237	0.
4.	H_L	48.954	54.122	58.788	42.566	0.
5.	S_L	-3.404	-3.404	-1.402	.300	0.
6.	ξ	-34.203	-30.842	-18.150	-2.971	0.

Table 15. Solution of Shell Stresses for $\frac{r}{t} = 200$

Row	Load	ϕ = 40°	30°	20°	10°	0
		Values of T_ϕ at $\frac{\ell}{2}$ (pounds per inch)				
1.	None					
2.	Dead	-39.463	-38.863	-37.083	-34.175	-30.229
3.	V_L	38.143	2.837	-59.109	-51.667	12.494
4.	H_L	-35.404	-7.549	45.175	54.141	17.737
5.	S_L	-.567	-.950	-.782	1.398	0
6.	ξ	-37.291	-44.525	-51.799	-33.099	0
		Values of S at 0 (pounds per inch)				
1.	None					
2.	Dead	0.	-8.712	-17.190	-25.122	-32.297
3.	V_L	0.	228.819	153.039	-212.808	0.
4.	H_L	0.	-180.470	-152.961	97.205	0.
5.	S_L	0.	1.925	-4.212	-8.520	32.297
6.	ξ	0.	41.553	-21.324	-149.245	0.
		Values of T_x at $\frac{\ell}{2}$ (pounds per inch)				
1.	None					
2.	Dead	-31.981	-31.507	-30.055	-27.687	-24.499
3.	V_L	1082.695	416.678	-994.090	-1189.954	4160.566
4.	H_L	-824.133	-379.464	613.330	900.359	-2609.105
5.	S_L	14.120	-6.136	-33.757	27.595	324.133
6.	ξ	240.701	-.429	-444.572	-289.687	1851.095
		Values of M_ϕ at $\frac{\ell}{2}$ (inch pounds per inch)				
1.						
2.						
3.	V_L	-26.685	-43.370	-68.007	-52.164	0.
4.	H_L	13.279	28.569	52.902	46.298	0.
5.	S_L	-2.002	-1.902	-1.201	0.	0.
6.	ξ	-15.408	-16.703	-16.306	-5.866	0.

Table 16. Tension Test on 3/8" O.D. Plastic Tube

Test A

Time	0	10 sec.	30 sec.	1 min.	2 min.	4 min.	Strain
Strain "/"	Stress #/□"						
.0	73.3						
.00053	334.1	325.9	322.7	314.5	309.6	301.5	
.00100	505.2	497.1	492.2	485.7	479.1	474.2	.00098
.00150	764.3	749.7	741.5	733.4	728.5	717.1	.00145
.00200	987.6	974.6	961.5	953.4	942.0	922.4	.00193
.00250	1212.5	1196.2	1183.2	1175.0	1158.7	1142.4	.00242
.00300	1443.9	Specimen broke. (Weakened by glue at end plug)					

Test B

Strain "/"	Stress #/□"
.0	0.
.00040	309.6
.00110	651.9
.00150	814.9
.00180	977.8
.00255	1303.8
.00325	1662.3
.00315	1548.2
.00210	994.1
.00130	668.2
.00065	350.4
.00025	163.0

Test C

Strain "/"	Stress #/□"
.00040	163.0
.00060	325.9
.00093	488.9
.00135	651.9
.00170	814.9
.00200	977.8
.00275	1303.8
.00350	1629.7
.00413	1955.6
.00490	2297.9
.00565	2623.8
.00350	1629.7
.00275	1140.8
.00235	977.8
.00160	651.9
.00090	325.9
.00015	0.

Table 17. Deflection Test Readings

Edge Member Deflection (Telescope)

Position	Vertical Displacement	Horizontal Displacement
0.500 ℓ	0.47"	0.29"
0.375 ℓ	0.42	0.25
0.250 ℓ	0.32	0.18
0.125 ℓ	0.15	0.08

Central Members - Vertical Displacement (Ames Dial)

Member E (Crown)		Member D		Member C	
Position	Displacement	Position	Displacement	Position	Displacement
0.50 ℓ	-0.047"	0.35 ℓ	0.005"	0.40 ℓ	0.157"
0.40 ℓ	-0.044	0.15 ℓ	0.009	0.20 ℓ	0.100
0.30 ℓ	-0.040	0.05 ℓ	0.003	0.10 ℓ	0.007
0.20 ℓ	-0.010				
0.02 ℓ	+0.003				

Key: Vertical Displacement - Positive Downward
Horizontal Displacement - Positive Inward

F I G U R E S

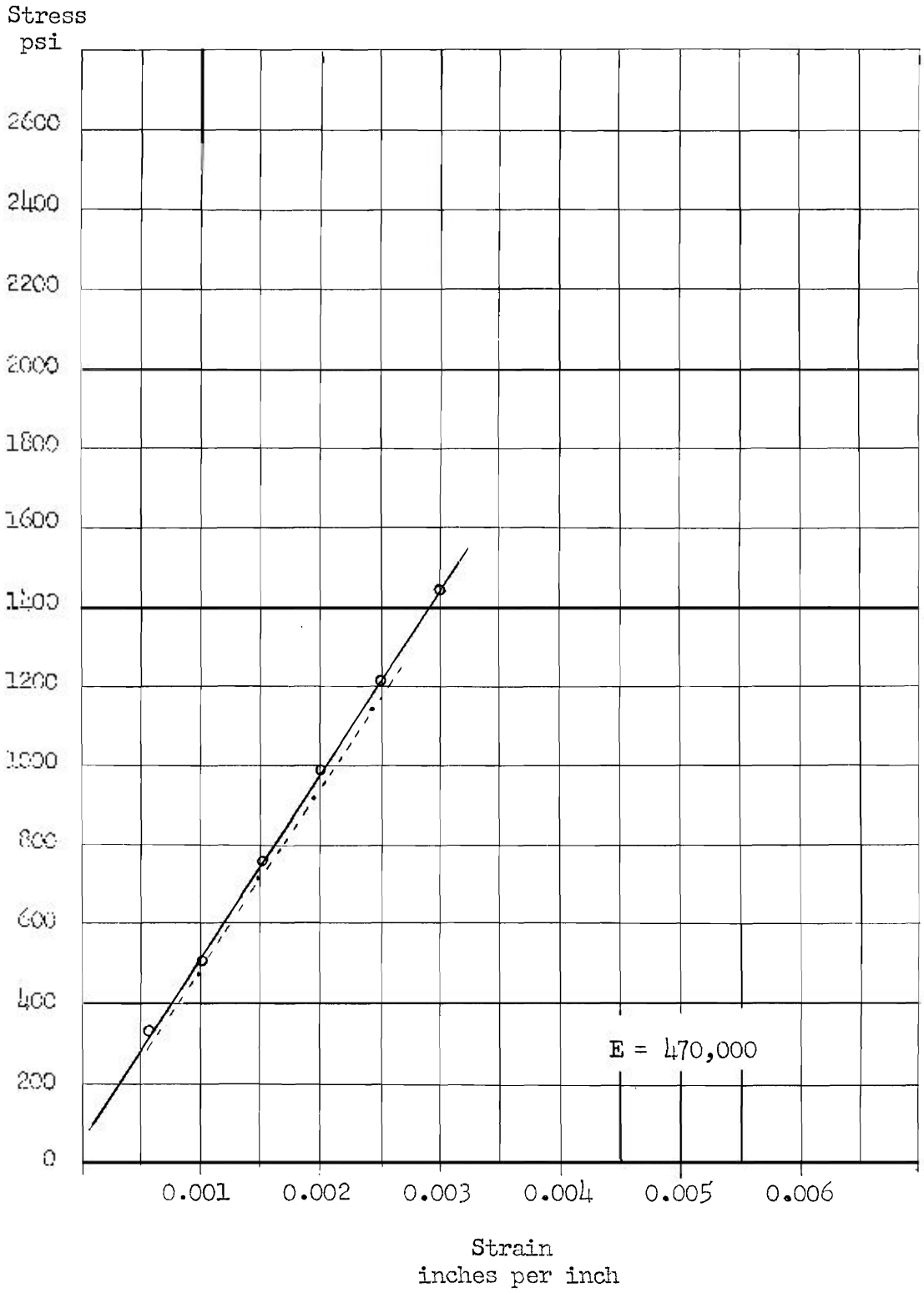

Figure 13. Stress - Strain Curve for Plastic Tube - Test A

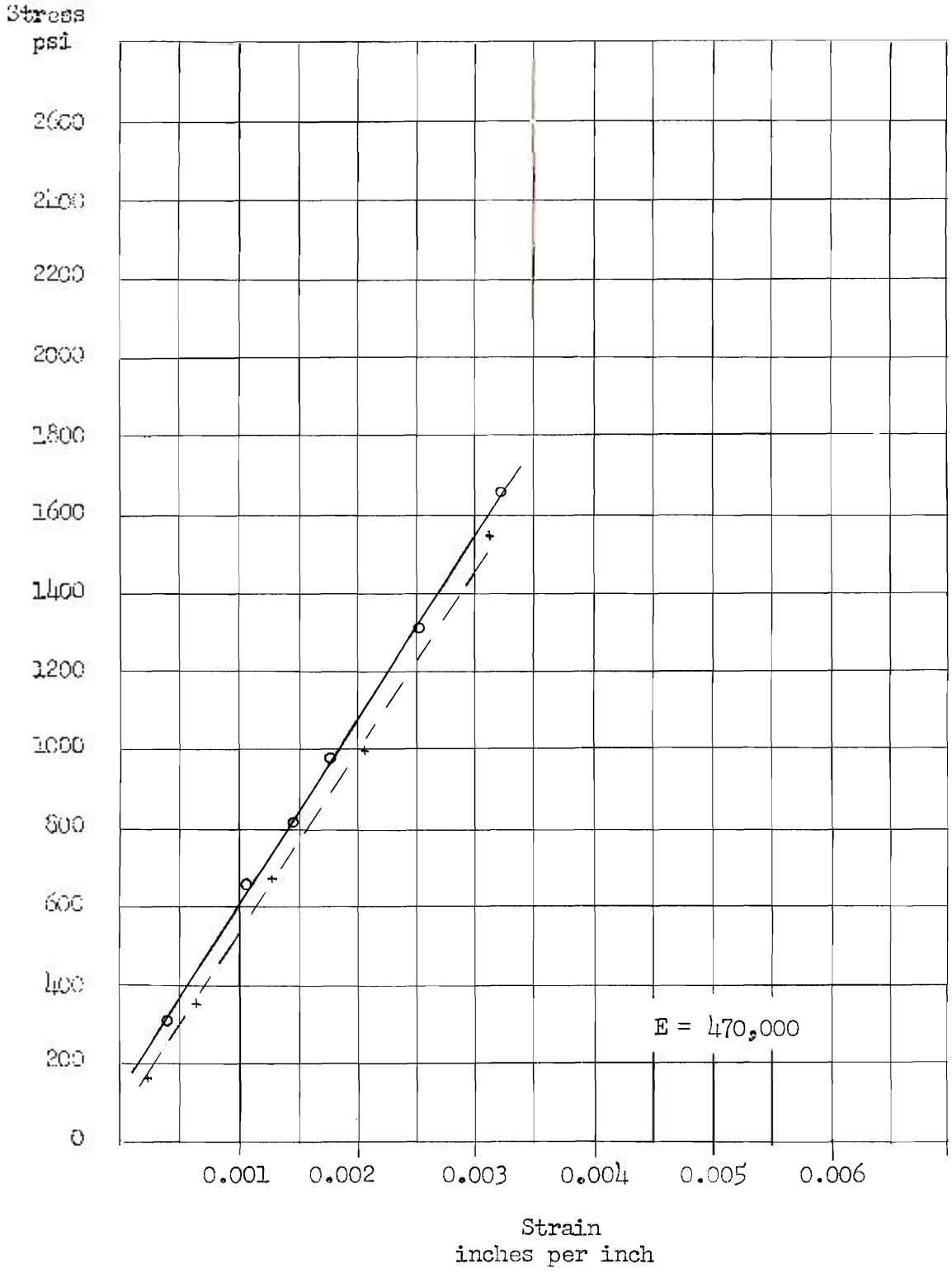

Figure 14. Stress - Strain Curve for Plastic Tube - Test B

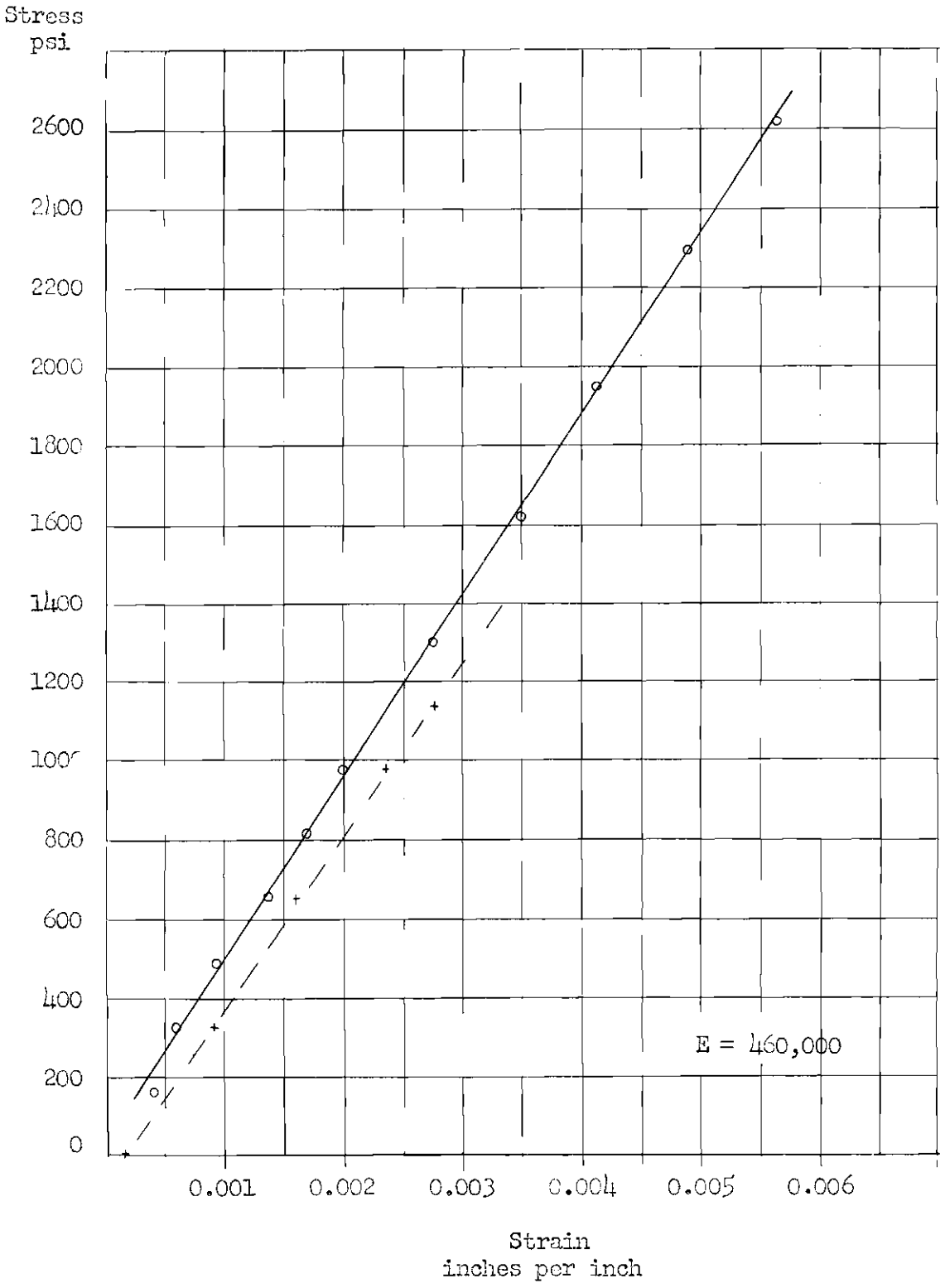

Figure 15. Stress - Strain Curve for Plastic Tube - Test C

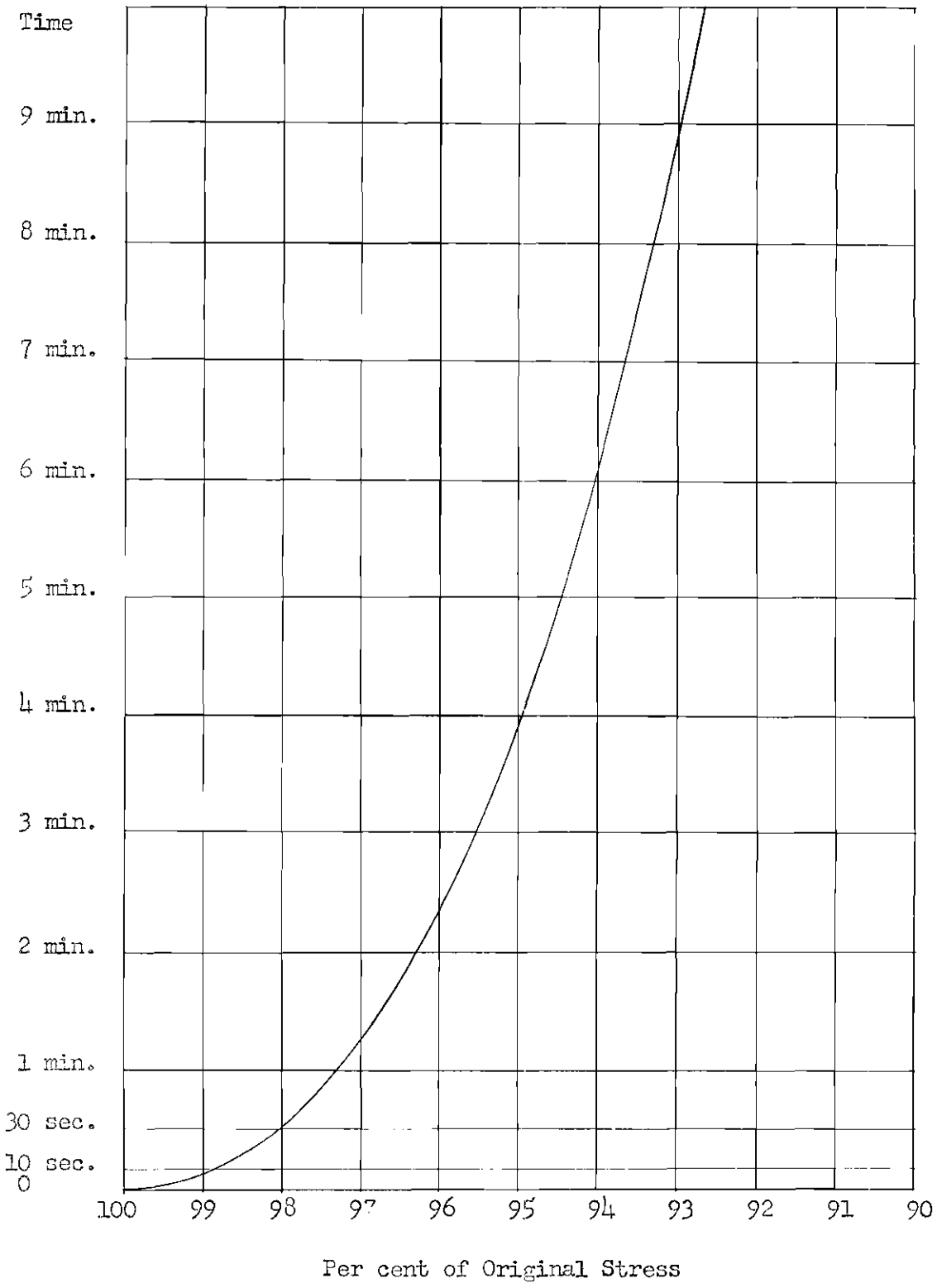

Figure 16. Creep of Plastic

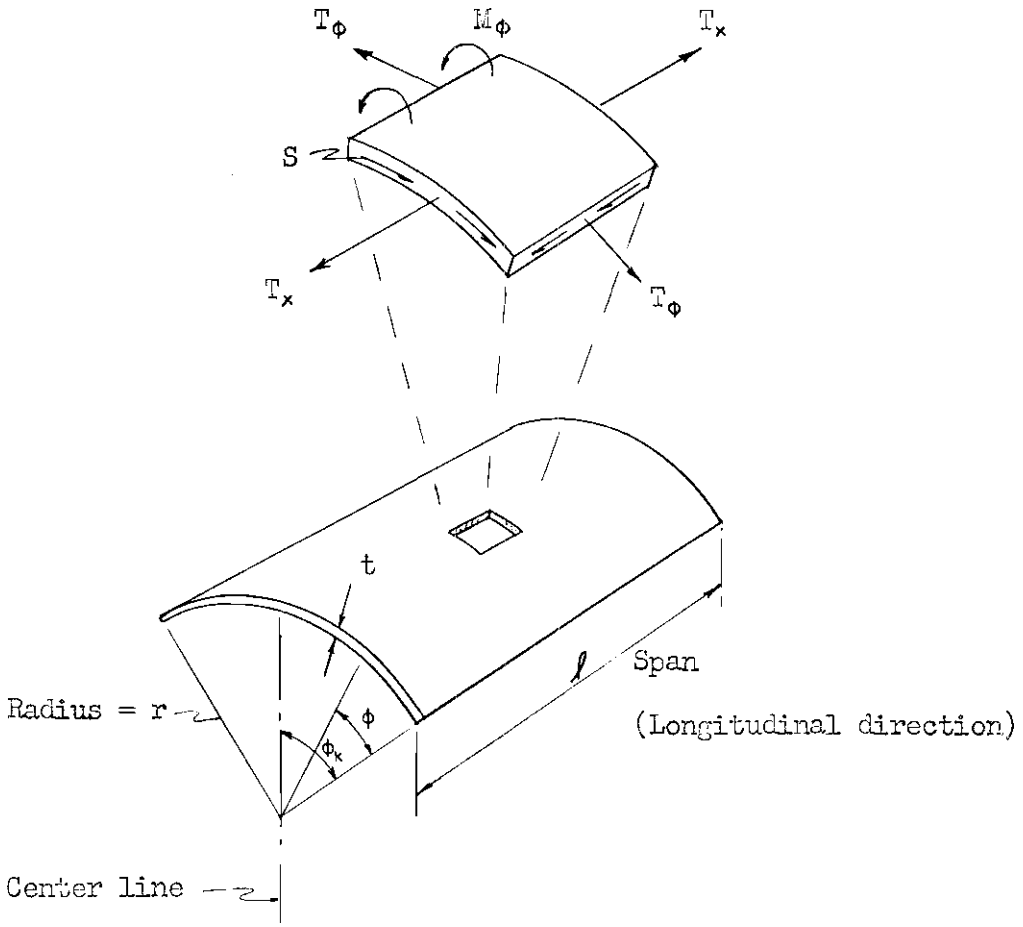

Figure 17. Shell Theory Notation

B I B L I O G R A P H Y

BIBLIOGRAPHY

1. Design of Cylindrical Concrete Shell Roofs, Manual No. 31, American Society of Civil Engineers, New York, 1952.

2. "Design of Barrel Shell Roofs", R/C 30, Portland Cement Association, Chicago, 1954.

3. Nervi, Pier Luigi, Structures, Trans. Giuseppina and Mario Salvadori, F.W. Dodge Corporation, New York, 1956.